CALPHAD: Computer Coupling of Phase Diagrams and Thermochemistry 91 (2025) 102888

Contents lists available at ScienceDirect

Calphad

journal homepage: www.elsevier.com/locate/calphad

Thermodynamics of the $MgCl_2$-$MgSO_4$ and $CaCl_2$-$CaSO_4$ systems

Amedeo Morsa [a,*], Elena Yazhenskikh [a], Rhys Dominic Jacob [a], Michael Müller [a], Dmitry Sergeev [a,b]

[a] Forschungszentrum Jülich GmbH, Institute of Energy Materials and Devices, Structure and Function of Materials (IMD-1), D-52425, Jülich, Germany
[b] NETZSCH-Gerätebau GmbH, D-95100, Selb, Germany

A B S T R A C T

Thermodynamic properties of $MgCl_2$-$MgSO_4$ and $CaCl_2$-$CaSO_4$ binary systems hold significant importance in the exploration of potential phase change materials for thermal energy storage applications. This study aims to elucidate the phase diagrams and thermodynamic properties of the eutectic mixtures within these systems, employing experimental techniques such as Differential Thermal Analysis (DTA) and Differential Scanning Calorimetry (DSC). Through comprehensive experimental investigations, the phase diagrams of the $MgCl_2$-$MgSO_4$ and $CaCl_2$-$CaSO_4$ systems were meticulously delineated, revealing the eutectic compositions and transition temperatures. Specifically, the eutectic composition for $MgCl_2$-$MgSO_4$ was proposed to be 28.0 mol% $MgSO_4$ with a melting temperature of 663 ± 5 °C, while for the $CaCl_2$-$CaSO_4$ system it was found to be at 14.0 mol% $CaSO_4$ and 722 ± 5 °C. Additionally, the enthalpy of fusion of these eutectic mixtures was for the first time determined, providing crucial insights into their thermal behaviour. They are 38.2 ± 1.0 kJ/mol for the Mg-containing system and 30.2 ± 0.4 kJ/mol for the Ca-containing system, respectively. The experimental data obtained in this study served as the foundation for the development of a new Gibbs energy dataset, which is essential for conducting thermodynamic calculations. The utilisation of this dataset enables accurate predictions of thermodynamic properties across the entire composition and temperature ranges of the systems under investigation.

1. Introduction

Renewable energy technologies play a crucial role in mitigating climate change and reducing reliance on fossil fuels [1]. Among them, concentrating solar power (CSP) represents a promising option for electricity generation, relying on solar heat as an abundant and renewable energy source [2]. CSP integrated with thermal energy storage (TES) is a technology that can provide dispatchable energy. It allows to correct the gap between the period of energy availability and its period of usage, by storing the sun's heat during the day-light and reusing it during the night. In the frame of thermal energy storage methods [3–6], latent heat thermal energy storage (LHS) involves using phase change materials (PCMs) that undergo phase transformations (solid-solid, solid-liquid and liquid-gas). The storage mechanism consists of heating a material until it experiences a phase change. A large number of materials are identified as suitable PCMs [3,7], among them inorganic salts [8,9]. Inorganic PCMs, despite their disadvantages related to corrosion and phase separation, show higher thermal conductivity and storage capacity than organic PCMs [10]. Among them, eutectic phase change materials (EPCMs), and more specifically molten salts, show superior performance in TES applications compared to single-component PCMs, with a larger phase change temperature range and higher phase stability [11]. Phase diagrams are essential for describing the relationship between the melting temperature and composition of potential PCMs.

Investigating the $MgCl_2$-$MgSO_4$ and $CaCl_2$-$CaSO_4$ systems provides valuable insights into their potential as promising PCMs for CSP and TES applications. Magnesium- and calcium-based salts have attracted increasing attention in the literature as suitable candidates, due to their low cost, availability, and favourable thermal properties [12–15]. The present study contributes to the characterisation of these systems as part of a broader effort to understand the thermodynamic behaviour of the reciprocal salt system Mg^{2+}, Ca^{2+}/Cl^-, SO_4^{2-} that is part of the salt database developed in the PCM project [16]. Thermodynamic properties of the chloride-sulphate systems are important for the identification of potential PCMs which satisfy key criteria for successful thermal energy storage, such as high latent heat of fusion, suitable phase change temperature range, thermal stability, and cost-effectiveness [7,17]. According to the CALPHAD methodology, the available experimental information (phase equilibria, thermodynamic properties) is used in order to generate a thermodynamic dataset containing the proper Gibbs energies for all phases in the system. Several studies have previously focused on nitrates, chlorides, and sulphates, aiming to establish a robust and comprehensive thermodynamic database for high-temperature thermal energy storage applications [12,15,18–20]. The present study contributes further to this ongoing effort by providing

* Corresponding author.
E-mail addresses: amedeomorsa@hotmail.it, a.morsa@fz-juelich.de (A. Morsa).

https://doi.org/10.1016/j.calphad.2025.102888
Received 30 July 2025; Received in revised form 11 September 2025; Accepted 7 October 2025
Available online 10 October 2025

new thermodynamic data specifically related to sulphate-containing systems. As demonstrated elsewhere [15], sulphates typically suffer from decomposition into oxides in open systems, significantly compromising their applicability as phase change materials. However, mixing sulphates with chlorides effectively lowers their melting temperatures. Thus, identifying eutectic mixtures characterised by intermediate melting points - lower than the decomposition temperatures of pure sulphates - offers a practical solution. This strategy circumvents the decomposition challenge and enables sulphate-based eutectic mixtures to be reconsidered as promising candidates for thermal energy storage applications.

The $MgCl_2$-$MgSO_4$ system was investigated by Jänecke [21], who identified it as a simple eutectic system with a eutectic temperature of 667 °C and a composition of 20 mol% of $MgSO_4$. Speranskaya [22] reported the eutectic at 656 °C and 22.5 mol% of $MgSO_4$. Both studies did not report any experimental data at high compositions of $MgSO_4$, due to the decomposition of sulphate above 1000 °C [23–25].

The $CaCl_2$-$CaSO_4$ system was investigated by several authors [26–32], but there is not a complete binary phase diagram for such a system. Sackur [26] reported a value of 727 °C at 14.4 mol percent of $CaSO_4$ as the minimum of the liquidus curve involving $CaCl_2$. Pichugin [27] studied the system in the composition range 0–25 mol% $CaSO_4$ and presented a eutectic at 718 °C and 15 mol%. Jänecke et al. [28] only reported, in the study of reciprocal system K^+, Ca^{2+}//Cl^-, SO_4^{2-}, that the eutectic is close to high $CaCl_2$ content. Golubeva et al. [29] reported a eutectic at 706 °C and 12.5 mol% $CaSO_4$. Palkin [30] and Zimina et al. [33] confirmed the same mole percentage with a temperature of 712 °C. Arbukhanova et al. [32] considered the same eutectic composition at 708 °C in their investigation of the ternary system CaF_2-$CaCl_2$-$CaSO_4$. They investigated only part of the composition range of the phase diagram due to the decomposition of $CaSO_4$ above 1200 °C [25,34], similar to the limitations observed previously for the magnesium-containing system.

To the best of the authors knowledge, no experimental data are currently available in the sulphate-rich region for the aforementioned systems, nor have enthalpy values been reported for the corresponding eutectic compositions. Therefore, the current study aims to perform detailed thermal analysis study on mixtures covering the entire composition range and to carry out calorimetric analyses for further reassessment and improvement of the thermodynamic database. This approach enables confirmation of the complete phase diagrams and provides a more accurate description of the systems. Furthermore, by applying the CALPHAD methodology, the improved dataset allows for reliable predictions of the behaviour of complex salt mixtures and the identification of new candidate materials for thermal energy storage applications.

2. Experimental

2.1. Samples

The pure compounds $MgCl_2$ (Sigma-Aldrich, anhydrous 99,99 %), $CaCl_2$ (Alfa Aesar, anhydrous 99,99 %), $MgSO_4$ (VWR Chemicals, anhydrous ≥99 %, metal basis) and $CaSO_4$ (Alfa Aesar, anhydrous 99,993 %) were used for the preparation of the mixtures. Before preparation, each powder underwent a drying treatment in a vacuum furnace at 150 °C for 24 h to ensure complete moisture removal. Subsequently, all sample handling and mixture preparations were performed inside a glove box ($O_2 < 0.5$ ppm, $H_2O < 1$ ppm) under a controlled, dry argon atmosphere to prevent moisture contamination. Mixtures, ranging between 50 and 100 mg, were accurately weighed and directly transferred into tube-shaped platinum crucibles according to the desired molar compositions. The determination of melting temperature of pure compounds and high sulphate content mixtures is hampered by decomposition of sulphates into their corresponding oxides before reaching their melting temperatures [23–25,34]. As previously demonstrated [15], significant mass losses of approximately 65.78 % and 58.80 % were recorded for $MgSO_4$ and $CaSO_4$, respectively, when heated above 1000 °C and 1200 °C in open crucibles. To circumvent the decomposition issues inherent in open systems, as demonstrated in our previous investigation [15], the studies were conducted in sealed platinum tubes in order to avoid any loss of SO_3 and to promote equilibrium within the crucible.

2.2. Instruments

2.2.1. Differential Thermal Analysis and Thermal Gravimetry (DTA/TG)

DTA measurements were performed using a STA 449 C Jupiter (Netzsch) with a silicon carbide oven (RT-1600 °C) and a sample holder with a type S thermocouple (Pt/(Pt10Rh)). The temperature calibration was conducted using the structure and phase transition temperatures of C_6H_5COOH (122.5 °C), $RbNO_3$ (164.2 °C), $KClO_4$ (300.8 °C), Ag_2SO_4 (462.2 °C), CsCl (470.0 °C), K_2CrO_4 (668.0 °C), $BaCO_3$ (808.0 °C), K_2SO_4 (1069.0 °C), and CaF_2 (1418.0 °C) in platinum tubes. The resulting accuracy of transition temperature measurements is ±5 °C. The experiments were carried out with a heating and cooling rate of 5 K/min and 3 cycles of heating and cooling under Ar atmosphere with a flow rate of 20 ml/min. All phase transition temperatures were determined with Proteus Analysis software from Netzsch. The results showed good reproducibility from the second cycle. In this work, the phase transition temperatures were primarily determined from the heating curves. Specifically, the onset temperature of the eutectic transformation was taken as the eutectic point, while the maximum peak temperature of subsequent thermal events was assigned to the liquidus or solid-solid transformation temperatures. In cases where the heat flow signals during heating were weak or broad, the corresponding transitions were instead identified from the cooling curves, provided that the latter exhibited sharper and more clearly defined peaks.

Due to sulphate decomposition, which can also occur to a small extent in closed crucibles until the decomposition pressure is reached, the experimentally measured melting temperatures of pure sulphate compounds may only represent a minimum. This is because the possible formation of metal oxides (MO, where M = Mg or Ca) can lower the liquidus temperature by effectively turning the system into a binary mixture (MO-MSO_4). The same applies to the mixtures of the binary system MCl_2-MSO_4, which would in turn become the ternary MCl_2-MO-MSO_4. In order to prevent mass loss due to decomposition of sulphates and vaporisation of chlorides, sealed platinum tubes with a height of 2 cm, a diameter of 5 mm and a wall thickness of 0.3 mm were used for analysis. The platinum crucible was closed after filling the sample (approximately 100 mg) under dry argon in a glove box and then welded outside the box in a hydrogen/oxygen flame.

2.2.2. Differential Scanning Calorimetry (DSC)

The determination of thermodynamic properties was carried out using two different differential scanning calorimeters. A differential scanning calorimeter DSC 404C Pegasus (Netzsch) with a Pt oven (RT-1500 °C) and a type S thermocouple (Pt/(Pt10Rh)) was used to determine the heat capacity of the eutectic mixtures. The temperature calibration was performed with the pure compounds C_6H_5COOH (122.5 °C), $RbNO_3$ (164.2 °C), $KClO_4$ (300.8 °C), Ag_2SO_4 (462.2 °C), CsCl (470.0 °C), K_2CrO_4 (668.0 °C), $BaCO_3$ (808.0 °C), K_2SO_4 (1069.0 °C), CaF_2 (1418.0 °C). The average temperature deviation was ±2 °C. Ar atmosphere with a gas flow of 20 ml/min was used. The sample powder of 30–40 mg was loaded into an alumina liner within the platinum pan, and was subjected to a heating rate of 10 K/min. The use of an alumina liner aimed to minimise material creeping and facilitate post-experimental sample handling. Although alumina may react with MgO and CaO - potential decomposition products of the investigated sulphates - this setup was considered acceptable since all experiments were conducted well below the decomposition temperature of the sulphates, thus avoiding the formation of these oxides and any secondary reactions

with the crucible material. A disc-shaped sapphire standard was used as the reference material. The C_p signals were evaluated using Netzsch analysis software. A Calvet-type DSC calorimeter, model mHTC 96 (Setaram), was used for comparison of the heat capacity of the eutectic compositions of the two systems under investigation with measurements obtained using the other calorimetric instrument. Additionally, this device was used to validate the fusion enthalpy of the pure magnesium chloride. The sample powder of 200–300 mg was loaded in alumina liner and platinum crucibles. The heating rate of 4 K/min under He with a flow of 5 ml/min was applied. The three-step ratio method [35] with sapphire (α-Al_2O_3, NIST Standard Reference Material SRM720, purity 99,95 %, metal basis) [36] as a reference was applied for the determination of the heat capacity (C_p°, J•mol^{-1}•K^{-1}) according to the following equation:

$$C_{p(s)}^{\circ} = \frac{m_r}{m_s} \cdot \frac{DSC_s - DSC_b}{DSC_r - DSC_b} \cdot C_{p(r)}^{\circ} \quad (1)$$

where m is the mass of the substance (g), DSC is the signal of thermopile (μV), and subscripts b, r and s stand for baseline, reference and sample respectively. Baseline and reference measurements were performed for each measured sample separately. The sapphire reference was a disc-shaped specimen of mass comparable to that of the sample mass under analysis.

2.2.3. X-ray diffractometry (XRD)

An Emperyean diffractometer from Malvern PANalytical equipped with a Cu-LFF X-ray tube (operated at 40 kV and 40 mA), BBHD mirror and a PIX-cel3D detector was used for XRD analysis. A continuous flow of synthetic air was applied during the experiment. Lattice parameters and amounts of secondary phases were determined through Rietveld refinement using the profile analysis software TOPAS version 6 from Bruker AXS. Crystal structures were obtained from the Inorganic Crystal Structure Database (ICSD). The uncertainty for molar volume was estimated to be ±0.02 cm^3/mol. XRD investigation was conducted on synthesised samples to verify their purity and identify any existing crystalline phases. The stoichiometric amounts of anhydrous pure

Table 1
Thermodynamic data of stochiometric compounds used in the present work.

Compound	$\Delta H^0_{298,f}$ J/mol	S^0_{298} J/mol•K	T (K)	C_p, J/mol•K	Ref.
$MgCl_2$ (solid)	−644300 [52]	89.62 [52]	1–40	0.01578312T–0.00540726797T^2 + 6.88028004•10^{-4}T^3 - 2.6046278•10^{-5}T^4 + 5.53055764•10^{-7}T^5 - 4.56290219•10^{-9}T^6	[16, 53]
			40–298	214.15146–1.3637537T + 204423.51T^{-2} + 0.0083405079T^2 - 2.53029383•10^{-5}T^3 - 2.90946621•10^{-8}T^4 - 11675.506/T	[16]
			298–987	75.65277 + 0.009980036T - 643923.9T^{-2} - 3.198664•10^{-9}T^2	[52]
			987–2900	84.782	[16]
$MgCl_2$ (liquid)	−609584.64 [16]	117.243 [16]	S→L ΔH_{tr} = 43.1 kJ/mol at 987 K (714 °C)		[16]
			1–40	0.01578312T–0.00540726797T^2 + 6.88028004•10^{-4}T^3 - 2.6046278•10^{-5}T^4 + 5.53055764•10^{-7}T^5 - 4.56290219•10^{-9}T^6	[16]
			40–117	214.15146–1.3637537T + 204423.51T^{-2} + 0.0083405079T^2 - 2.53029383•10^{-5}T^3 - 2.90946621•10^{-8}T^4 - 11675.506/T	[16]
			117–2900	92.048	[16]
$CaCl_2$ (solid)	−795797 [46]	104.602 [46]	1–50	0.78155423–0.12359292T + 0.0306270316T^2 - 3.49282014•10^{-4}T^3	[48]
			50–180	−16.732490 + 1.1686419T - 6.02988655•10^{-3}T^2 + 1.1662759•10^{-5}T^3	[48]
			180–600	43.925204 + 0.17176775T - 3.10281876•10^{-4}T^2 + 1.97728035•10^{-7}T^3	[48]
			600–1045	77.936089–0.00630254569T + 6.57695848•10^{-6}T^2 + 7.52474113•10^{-9}T^3	[48]
			1045–3000	87.12	[48]
$CaCl_2$ (liquid)	−786860.75 [48]	104.602 [48]	S→L ΔH_{tr} = 28.543 kJ/mol at 1045 K (772 °C)		[46]
			1–50	0.78155423–0.12359292T + 0.0306270316T^2 - 3.49282014•10^{-4}T^3	[48]
			50–180	−16.732490 + 1.1686419T - 6.02988655•10^{-3}T^2 + 1.1662759•10^{-5}T^3	[48]
			180–486	43.925204 + 0.17176775T - 3.10281876•10^{-4}T^2 + 1.97728035•10^{-7}T^3	[48]
			486–3000	116.0	[48]
$MgSO_4$ (LT)	−1288800 [52]	91.6 [52]	1–42	8.73213058•10^{-5}T^3	[20]
			42–298	10.582036 + 0.44690916T + 34086.236T^{-2} – 4.7507286•10^{-4}T^2 - 1740.55857/T	[20]
			298–1283	85.18297 + 0.08756883T - 1167240T^{-2} – 1.982192•10^{-5}T^2	[52]
			1283–2000	155	[52]
$MgSO_4$ (HT)	−1274200 [15]	102.828 [15]	LT→HT ΔH_{tr} = 14.6 kJ/mol at 1300.3 K (1027.1 °C), C_p like $MgSO_4$ (LT)		[15]
$MgSO_4$ (liquid)	−1238766 [15]	120.880 [15]	HT→L ΔH_{tr} = 43.4 kJ/mol at 1410.2 K (1137.0 °C)		[15, 52]
			1–42	8.73213058•10^{-5}T^3	[20]
			42–298	10.582036 + 0.44690916T + 34086.236T^{-2} – 4.7507286•10^{-4}T^2 – 1740.55857/T	[20]
			298–1283	85.18297 + 0.08756883T–1167240T^{-2} – 1.982192•10^{-5}T^2	[52]
			1283–2000	155	[52]
$CaSO_4$ (LT)	−1437622 [52]	107.492 [54]	1–39	1.58639676•10^{-4}T^3	[20]
			39–298	60.2427676 + 0.22021804T + 73416.5259T^{-2} - 1.3048247•10^{-4}T^2 - 4185.07635/T	[20]
			298–1784	100.854288 + 0.06896988T - 1736052.08T^{-2} - 8.6603105•10^{-6}T^2	[20]
			1784–2000	195.63	[15]
$CaSO_4$ (HT)	−1420012 [20]	119.282 [20]	LT→HT ΔH_{tr} = 17.6 kJ/mol at 1493.6 K (1220.4 °C), C_p like $CaSO_4$ (LT)		[15, 20]
$CaSO_4$ (liquid)	−1425938 [20]	107.714 [15]	HT→L ΔH_m = 16 kJ/mol at 1783.6 K (1510.4 °C)		[15, 20]
			1–39	1.58639676•10^{-4}T^3	[20]
			39–298	60.2427676 + 0.22021804T + 73416.5259T^{-2} - 1.3048247•10^{-4}T^2 - 4185.07635/T	[20]
			298–795	100.854288 + 0.06896988T - 1736052.08T^{-2} - 8.6603105•10^{-6}T^2	[20]
			795–2000	195.63	[20]

compounds forming the mixture were thoroughly mixed, grinded in an agate mortar and heated up to 800 °C for 60 h in a sealed quartz ampoule. The resulting powder was reground and analysed by X-ray diffraction.

3. Thermodynamic modelling

3.1. Thermodynamic data of stochiometric compounds

Thermodynamic data (standard enthalpy of formation and standard entropy, $\Delta H^0_{298,f}$, S^0_{298}, and heat capacity as function of T, C_p(T), for pure solid and liquid compounds are summarised in Table 1, along with transition temperatures and heats of transitions. While this work does not involve Gibbs energy modelling of pure compounds, it utilises properties detailed in Table 1. Instead, a significant aspect of this study focuses on modelling the Gibbs energy for liquid solutions. This modelling approach, based on the Calphad method [37], is implemented using the FactSage software [38,39].

3.2. Thermodynamic model for liquid phase

The Gibbs energy of the liquid phase in the system was modelled using the modified non-ideal associate species model proposed by Besmann et al. [40], which has demonstrated applicability for complex oxide [41] and salt liquids [18,19]. The liquid phase was considered as an oxide-chloride solution to keep consistence with the general database. The pure compounds, MCl_2 and MSO_4 (M = Mg and Ca), in liquid phase, were taken as solution components. The interactions between them are responsible for the thermodynamic properties of the liquid phase. To provide equal weighting of each associate species with regard to its entropic contribution in the ideal mixing term in the oxide database, each species contains a total of two non-oxygen atoms per formula unit according to the model used by Besmann et al. [40]. For magnesium chloride, calcium chloride, magnesium sulphate and calcium sulphate, this was represented by ($MgCl_2$):1.5, $MgSO_4$, ($CaCl_2$):1.5 and $CaSO_4$, respectively, meaning that each atom stoichiometry for both chlorides is divided by 1.5. This has been done to provide compatibility with the general oxide database GTOx [42]. In addition, interactions between associate species were introduced in order to fine tune the thermodynamic description. The molar Gibbs energy of the solution is expressed as a three-term expression, comprising the reference term, the ideal mixing contribution and the excess part that accounts for binary interactions, as detailed below:

$$G_m = \sum x_i {}^{\circ}G_i + RT\sum x_i \ln x_i + \sum\sum_{i<j} x_i x_j \sum_{\nu=0} L_{ij}^{(\nu)}\left(x_i - x_j\right)^{\nu} \quad (2)$$

where x_i is the mole fraction of phase constituent i (including the associate species), ${}^{\circ}G_i$ is the molar Gibbs energy of the pure (liquid) phase constituent i and $L_{ij}^{(\nu)}$ with $\nu = 0, 1$ are the interaction coefficients between components i and j, according to the Redlich-Kister polynomial. ${}^{\circ}G_i$ and $L_{ij}^{(\nu)}$ are temperature dependent in the same way according to Equation (3):

$${}^{\circ}G_i, L_{ij}^{(\nu)} = A + BT + CT\ln(T) + DT^2 + ET^3 + F/T \quad (3)$$

Typically, in Equation (3), the optimisation process focuses primarily on the coefficients A and B.

3.3. Assessment of Gibbs energy parameters

The assessment of each of the two binary systems presented in this study was conducted by combining the experimental results obtained in the present work with available literature data on phase diagrams and thermodynamic properties. The various binary interaction parameters ($L_{ij}^{(\nu)}$) between species in the liquid solution were optimised. The C_p functions of all substances were assessed before the optimisation and kept constant. The selected solution parameters were optimised using the CALPHAD Optimizer module included in the FactSage software [38, 39,43], based on the available experimental data, which included both literature values and measurements obtained in this work.

4. Experimental results and discussion

4.1. Pure components

4.1.1. $MgCl_2$

In this work, the melting temperature of the pure magnesium chloride was validated through DTA measurements, with the aim of confirming and comparing them with available literature data. The experiments were performed in sealed platinum tubes, yielding a melting temperature of 719 °C (992 K), and the corresponding heating and cooling DTA curves are displayed in Fig. S 1. DSC measurements were performed to determine the enthalpy of fusion and to validate or refine the values reported in the literature. Two measurements were conducted employing a Setaram DSC instrument using alumina liners placed inside platinum crucibles covered with platinum lids (Fig. S 2). No mass loss was detected within the investigated temperature range, spanning from ambient temperature up to 780 °C. The melting temperature of pure $MgCl_2$, as measured by DSC tests, was 717 °C (990 K). The measured melting points of $MgCl_2$ (DTA: 719.4 ± 5 °C; DSC: 717 ± 2 °C) slightly exceed the commonly accepted value of 714 °C (987 K) [44–47]. This discrepancy is within the experimental uncertainty, and the value of 714 °C (987 K) adopted in the current database has therefore been maintained. The corresponding enthalpy of fusion obtained from integration of the heat capacity curves was 44.4 kJ/mol, while the value obtained from heat calibration at phase transition temperatures of reference materials was 41.9 kJ/mol. Taking the average of the two, the resulting enthalpy of fusion is 43.1 ± 1.3 kJ/mol (Table 2), which shows good agreement with literature data [44–47]. Given the agreement with values previously reported in the literature and already adopted in the current thermodynamic database, the calorimetric measurements obtained in this study served as a validation of the existing thermodynamic properties. As such, no modifications to the database have been made.

4.1.2. $CaCl_2$

The thermodynamic assessment of $CaCl_2$, previously carried out by Reis [48], has been adopted in the present work. That assessment combined calorimetric heat capacity measurements performed above and below the melting point with literature data [46], which were also used to support extrapolations of the liquid phase below the melting point and the solid phase at low temperatures. The standard formation enthalpy, standard entropy and heat capacity are collected in Table 1. The thermodynamic properties adopted in this work are summarised in Table 2. In the present study, the melting temperature was experimentally validated by DTA in sealed platinum tubes to ensure consistency with the rest of the DTA measurements. The measured melting point was 776 °C (1049 K), and the corresponding thermal curves are shown in Fig. S 3. This result is in good agreement with the literature values [49–51], and used in the working thermodynamic database (Table 2).

4.1.3. $MgSO_4$

The solid-solid transition and melting temperatures of the $MgSO_4$ compound were determined in a previous study [15] and are adopted in the present work. DTA measurements were performed in sealed platinum tubes, enabling heating to high temperatures without any mass loss. The observed transition and melting temperatures were 1027 °C (1300 K) and 1136 °C (1409 K), respectively. As previously reported [15], the corresponding enthalpy changes were measured by DSC, yielding values of 14.6 kJ/mol and 43.4 kJ/mol, which were used to update the thermodynamic database. The adopted values, based on these experimental results, are summarised in Table 2.

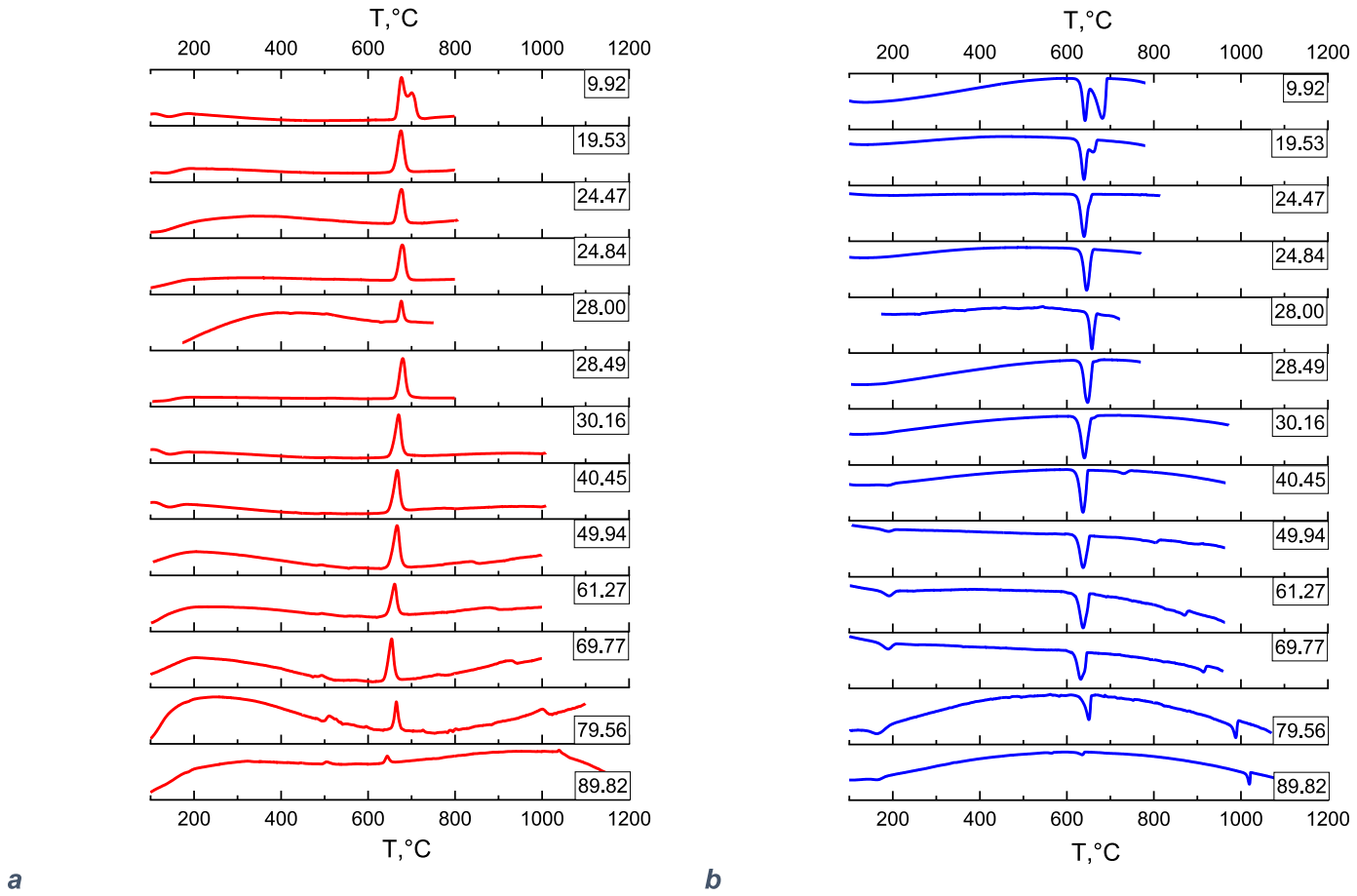

Fig. 1. DTA curves of $MgCl_2$-$MgSO_4$ mixtures, expressed in molar percentage of $MgSO_4$: **a** heating curves; **b** cooling curves.

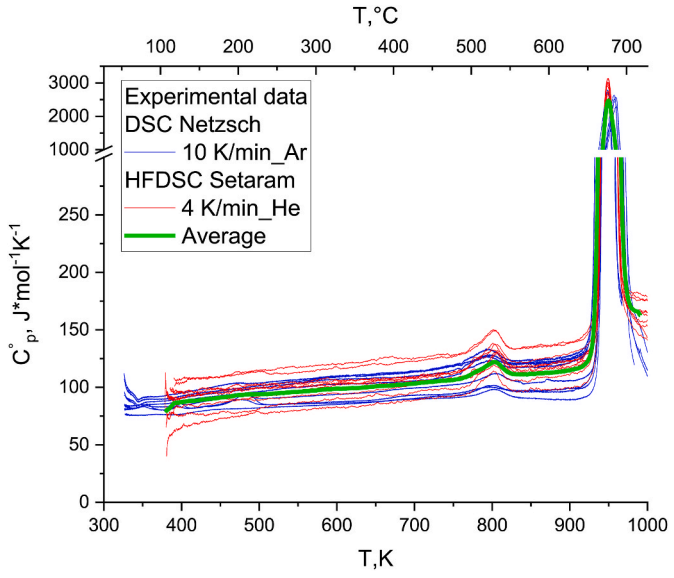

Fig. 2. Experimental values of molar heat capacity for solid and liquid phases of the $MgCl_2$(72.0 mol%)-$MgSO_4$(28.0 mol%) mixture measured by two DSC devices.

4.1.4. $CaSO_4$

Transition data for pure calcium sulphate were obtained from previous thermal analysis studies [15]. Solid-solid and solid-liquid transitions were identified at 1220 °C (1493 K) and 1510 °C (1783 K), respectively, based on DTA measurements conducted in sealed platinum tubes to ensure thermal stability and prevent mass loss. In that study, only the enthalpy of the solid-solid transition was measured calorimetrically by DSC, yielding a value of 17.7 kJ/mol. A summary of the adopted thermodynamic parameters is provided in Table 2.

4.2. $MgCl_2$-$MgSO_4$ system

DTA was employed in order to experimentally construct the phase diagram of the system under investigation and to validate it against existing literature data [21,22]. The use of sealed platinum crucibles made it possible to overcome the problem of sulphate decomposition and the influence of moisture on samples and to investigate the full range of phase diagram compositions, including high-sulphate-content regions not previously covered by other studies [21,22]. Additionally, preliminary DTA measurements were carried out in open alumina crucibles on five mixtures with low sulphate content, near the presumed eutectic composition. These preliminary tests revealed minor mass losses, as the maximum temperature investigated was below the decomposition temperature, highlighting the necessity of conducting experiments in closed systems. The corresponding DTA curves are provided in the supplementary materials (Fig. S 4).

For the construction of the phase diagram of the $MgCl_2$-$MgSO_4$ system, the transition temperatures were determined from the second heating of the DTA experiments. Thirteen mixtures covering the entire composition range were analysed in sealed platinum tubes placed in alumina crucibles. The DTA curves are shown in Fig. 1 and the corresponding transition temperatures listed in Table 3. In general, the temperatures in heating and cooling coincided within a range of ±5 °C, confirming that there was no supercooling in the cooling cycles. In the

Table 2
Transition data of pure compounds.

Reaction	Reaction Type	Temperature of transition		Heat of transition	
		T_{tr}, °C (K)	Ref.	ΔH_{tr}, kJ/mol	Ref.
$MgCl_2$					
$MgCl_2 \leftrightarrow$ liquid	melting	714 (987)	[44–47]	43.095	[44–47]
		712.7 (985.9)	[55]		
		719.4 (992.5)	a		
		716.7 (989.9)	b	43.1	b
$CaCl_2$					
$CaCl_2 \leftrightarrow$ liquid	melting	772 (1045)	[49–51]	28.543	[49–51]
		771.7 (1044.9)	[55]		
		776 (1049)	a		
$MgSO_4$					
$MgSO_4$ (LT) ↔ $MgSO_4$ (HT)	solid↔solid	1010 (1373)	[56]		
		997-1095 (1270–1368)	[25]		
		1010 (1283)	[20,38,52]	3	[38,45,52]
		1027.1 (1300.3)	[15],[a]		
		1029.9 (1303.1)	[15]	14.6	[15]
$MgSO_4$ (HT) ↔ liquid	melting	1124 (1397)	[23]		
		1120 (1393)	[24]		
		1185 (1458)	[57]		
		1136 (1409)	[25]		
		1137 (1410)	[20,45,52]	14.6	[20,52]
		1137 (1410)	[38]	23.6	[38]
		1135.6 (1408.8)	[15],[a]		
		1135.7 (1408.9)	[15]	43.4	[15]
$CaSO_4$					
$CaSO_4$ (LT) ↔ $CaSO_4$ (HT)	solid↔solid	1196 (1469)	[58]		
		1195 (1468)	[25,34,59]		
		1199 (1472)	[60]	29.43	[60]
		1211 (1484)	[61]		
		1201 (1474)	[62]	9.12	[62]
		1200 (1473)	[38,52]	5	[38,52]
		1227.4 (1500.6)	[20,63]	17.61	[20,63]
		1220.4 (1493.6)	[15],[a]		
		1222.6 (1495.8)	[15]	17.7	[15]
$CaSO_4$ (HT) ↔ liquid	melting	1380 (1653)	[59]		
		1450 (1723)	[58]		
		1462 (1735)	[34]		
		1528 (1801)	[64]		
		1506.8 (1779.9)	[63]		
		1460 (1733)	[52]	25.4	[52]
		1527 (1800)	[38]	36.84	[38]
		1506.8 (1779.9)	[20,63]	16	[20,63]
		1510.4 (1783.6)	[15],[a]		

[a] This work, DTA in sealed platinum tube.
[b] This work, DSC in open platinum crucible.

near eutectic composition region, it was not possible to discriminate from the heating curve whether the mixture under investigation was the eutectic, but only from the cooling curve, which instead showed a splitting of the signal into two peaks, eutectic and liquidus, respectively. For mixtures with high sulphate content, the high-temperature transition peak associated with the liquidus became progressively broader, weaker, and less defined in the heating curves. In contrast, the same transition appeared much sharper and more intense in the cooling curves. Nevertheless, in this study, transition temperatures were predominantly derived from the heating curves to avoid potential underestimation due to potential supercooling effects. Furthermore, these mixtures showed eutectic temperature at lower values than those reported in low-sulphate mixtures. During DTA measurements, a weak endothermic peak around 500 °C was observed in some of the high-sulphate compositions analysed. This peak was detectable exclusively during heating cycles and completely absent during cooling cycles. Subsequent experimental tests demonstrated that when the mixtures were analysed in open crucibles - which allowed for evaporation of contaminants at temperatures lower than the melting points of the mixtures - the peak completely disappeared after the first heating/cooling cycle. Additionally, X-ray diffraction analyses were conducted on three selected compositions (28, 50 and 90 mol% $MgSO_4$), to investigate the presence of intermediate compounds or secondary phases potentially forming in the system. The detailed XRD patterns and further analyses are provided in the supplementary material. The XRD results showed no evidence of contaminants, presumably originating from $MgSO_4$, that could explain the observed thermal effect. Moreover, the presence of MgO was found to be negligible (0.2 wt%, Fig. S 5) and insufficient to justify the appearance of an additional peak at around 500 °C or the observed lowering of the eutectic temperature by approximately 10 °C. Therefore, given the likely origin of these peaks as artefacts due to removable of contamination, these thermal events were excluded from consideration when constructing and assessing the phase diagram of the binary system investigated in this study.

DTA measurements indicated that the eutectic point is located at a composition near 28 mol% $MgSO_4$ and at 668 °C (941 K). The eutectic point is shifted toward higher sulphate concentrations compared to previous reports [21,22]. As a result, the liquidus line (liquid ↔ liquid + $MgSO_4$) on the sulphate-rich side of the eutectic composition exhibits a downward shift, leading to lower liquidus temperatures for these compositions. The solid-solid transition temperature of pure $MgSO_4$ was previously determined by the authors as 1027 °C (1300 K) in an earlier study [15].

4.2.1. *Thermodynamic properties of the eutectic mixture*

To bolster the evidence for the assessment of the $MgCl_2$-$MgSO_4$

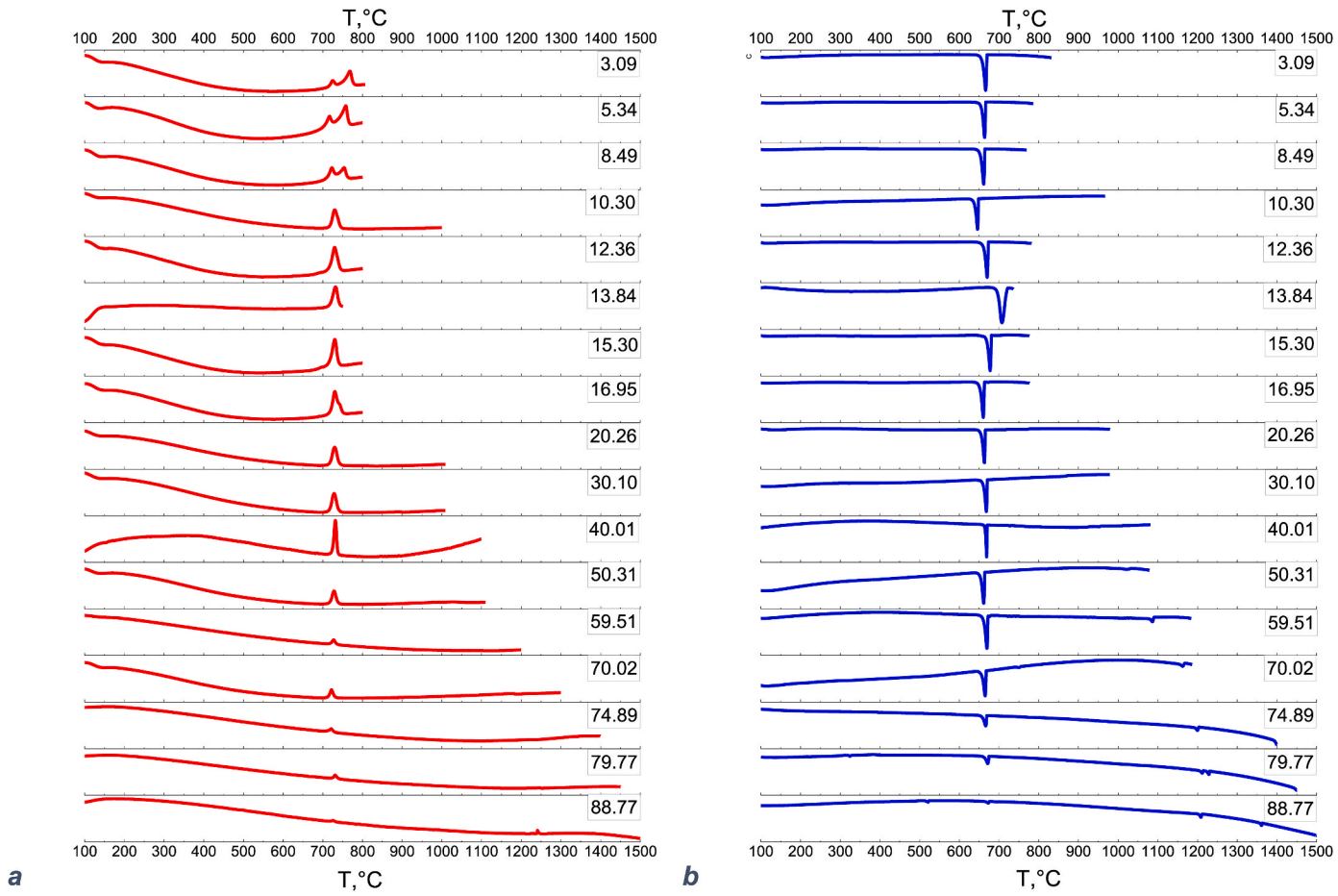

Fig. 3. DTA curves of $CaCl_2$-$CaSO_4$ mixtures, expressed in molar percentage of $CaSO_4$: **a** heating curves; **b** cooling curves.

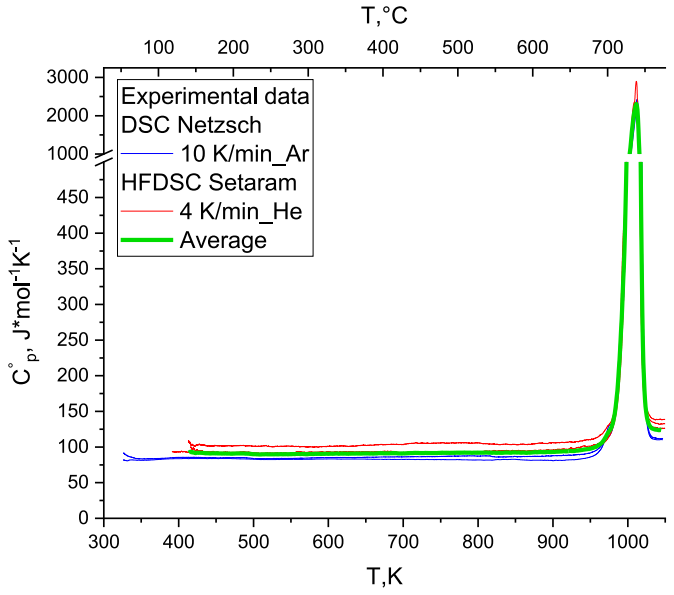

Fig. 4. Experimental values of molar heat capacity for solid and liquid phases of the $CaCl_2$(86.0 mol%)-$CaSO_4$(14.0 mol%) mixture measured by two DSC devices.

system, the assumed eutectic mixture $MgCl_2$(72.0 mol%)-$MgSO_4$(28.0 mol%) was chosen for further experimental determination of heat capacity and fusion enthalpy.

Table 3
Experimental DTA values of phase transition temperatures (°C) in the $MgCl_2$-$MgSO_4$ system.

$MgSO_4$, mol%	$MgSO_4$, wt%	Eutectic line	Liquidus line	Solid transition
0	0		719	
9.92	12.22	664	700	
19.53	23.48	659	669[a]	
24.47	29.06	650	658	
24.84	29.47	664		
28.00	32.96	668		
28.49	33.50	665		
30.16	35.31	654	674	
40.45	46.20	651	744[a]	
49.94	55.78	651	827	
61.27	66.67	647	878	
69.77	74.48	641	930	
79.56	83.11	657	979	
89.82	91.77	636	1035	
100	100		1136	1027

[a] From cooling curves.

The eutectic mixture has been synthesised *in situ*. The stoichiometric amount of anhydrous $MgCl_2$ (72.0 mol%) and $MgSO_4$ (28.0 mol%)[1] were thoroughly mixed and ground in an agate mortar in a glove box under argon atmosphere and heated up to 800 °C for 60 h in sealed quartz ampoule. The prepared sample was loaded in DSC Netzsch and Setaram crucibles for calorimetric tests.

[1] For all calculations the molar mass M = 102.26 g/mol of the $MgCl_2$(72.0 mol%)-$MgSO_4$(28.0 mol%) mixture was used.

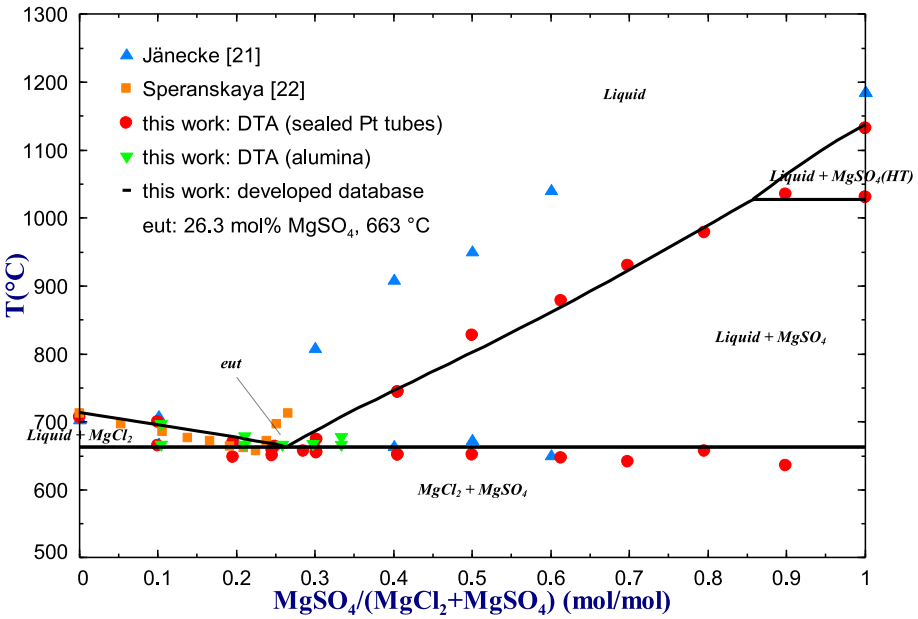

Fig. 5. Phase diagram of the $MgCl_2$-$MgSO_4$ system: comparison of experimental data of the present work with literature data [21,22] and the developed database.

The heat capacity of the eutectic mixture was measured in the temperature range from 50 °C to 750 °C by two DSC devices (described in section 2.2.2) with different heating rates (10 and 4 K/min). A total of ten samples from the same batch were analysed: three samples were heated from 50 °C to 700 °C, and seven from 50 °C to 750 °C, until their melting points were reached. The observed mass loss after heating up to 750 °C remained below 5 % (4.2 %).

The first DSC heating curve was disregarded due to its influence on removing water of crystallisation and the potential occurrence of a peak around 220 °C (493 K), which was attributed to the loading of the crucible onto the sample carrier. Such a peak was only present during the first heating cycle and disappeared thereafter. Therefore, for subsequent analyses, only the second and third curves were considered, with the first one indicating a drying process. Although the samples were initially dry, they may have absorbed some moisture during handling. As mentioned in section 4.2, DTA analyses had already revealed the presence of a peak at approximately 500 °C, which was not entirely clarified by XRD investigations. DSC measurements confirmed the presence of such a peak in the eutectic mixture. Unlike DTA analysis, which only detected this peak in mixtures with a medium to high sulphate content, DSC technique enabled its identification in mixtures with a low sulphate content, such as the eutectic mixture. DSC heating curves showed such a peak, which was not present in cooling curves. It is not clear if it refers to any phase transition. The assumption that it could come from the decomposition of $MgSO_4$ is unlikely, considering that sulphate decomposition occurs at temperatures above 1000 °C. Additionally, XRD investigation of the eutectic mixture did not prove the presence of any additional phase other than pure compounds in their weight ratio (Fig. S 5).

The eutectic melting temperature obtained from DSC analysis was found to be 663 °C (936 K), showing fair agreement with the value of 668 °C (941 K) determined from DTA measurements. The C_p curves are illustrated in Fig. 2. As noted elsewhere [12], varying heating rates do indeed impact the width of the phase transition range, as illustrated in this case (Fig. 2). However, the heat capacities of the liquid and solid phases exhibit consistency with each other. Creeping effects of the molten salts were observed during the measurements. Although they did not compromise the reliability of the analysis, they were detectable in the C_p curves recorded with the Netzsch calorimeter (blue curves in Fig. 2). In particular, the reduced height of the crucible may have contributed to this effect, especially in the liquid region where salt mobility increases. The coefficients derived from the measured heat capacity are presented in Table 4.

Integration of the peak area of phase transition gives the value of enthalpy of fusion. It is 37.1 kJ/mol from DSC 404C (10 K/min) and 39.3 kJ/mol from mHTC 96 (4 K/min). The mHTC 96 device was also calibrates with fusion enthalpies of reference material through the determination of the area under the phase transition curve. Utilising this approach, the enthalpy of fusion, averaged across the five samples under examination, is determined to be 37.64 kJ/mol. This calibration method is fully equivalent to the C_p curve integration method, as evidenced by the very close agreement between the values obtained from both approaches, with values of 37.6 ± 2.7 kJ/mol from the calibration method and 38.2 ± 1.1 kJ/mol as the average from the integration method of both DSC devices. The resulting weighted average value of the two, considered in this work as the final experimental value of enthalpy of fusion of the eutectic point, is 38.2 ± 1.0 kJ/mol.

4.3. $CaCl_2$-$CaSO_4$ system

The phase diagram of the $CaCl_2$-$CaSO_4$ system has been studied experimentally several times [26–32], but in all cases without offering a complete phase diagram covering the high sulphate region. Preliminary DTA experiments conducted in open alumina crucibles on mixtures with compositions close to the eutectic (up to 900 °C), shown in Fig. S 6, exhibited mass losses lower than 3 wt%. These preliminary results indicated that partial investigation of the system in open DTA crucibles is feasible without significant interference from mass loss. Nevertheless, to achieve better resolution of thermal effects and to ensure consistency and reliability of measurements, only results from sealed platinum crucibles are presented and discussed in this work. Seventeen compositions were analysed and the resulting DTA curves are shown in Fig. 3,

Table 4
Coefficients of the molar heat capacity ($J \bullet mol^{-1} \bullet K^{-1}$) $C_p^\circ = A + B \cdot T + C \cdot T^{-2} + D \cdot T^2$ for the $MgCl_2$(72.0 mol%)-$MgSO_4$(28.0 mol%) mixture taken from DSC measurements.

Temperature range/K	A	B	C	D
298–936	48.96872	$7.975 \bullet 10^{-2}$	$1.167316 \bullet 10^{6}$	$-1.72591 \bullet 10^{-5}$
936–1050	165.1			

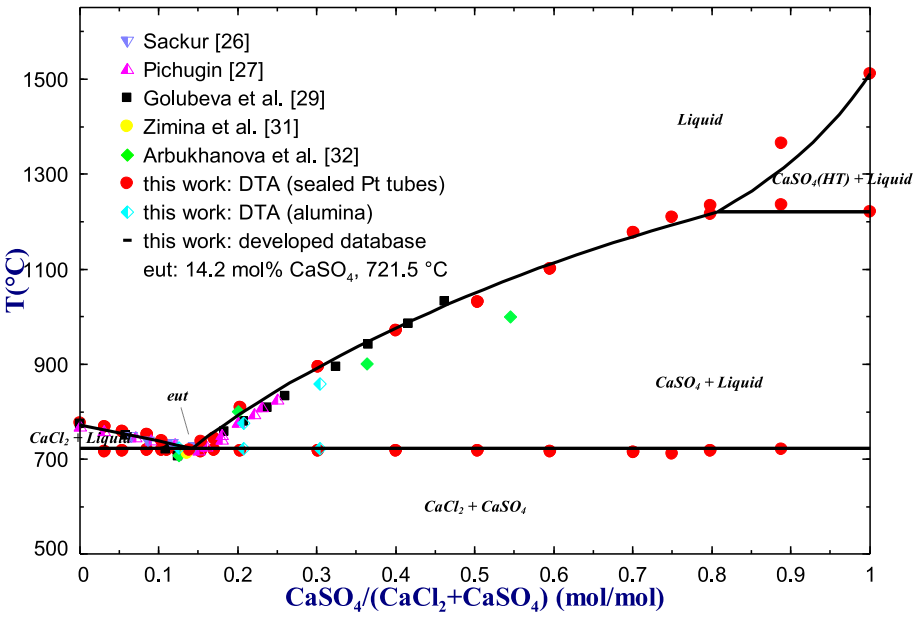

Fig. 6. Phase diagram of the $CaCl_2$-$CaSO_4$ system: comparison of experimental data of the present work with literature data [26,27,29,31,32] and the developed database.

Table 5
Experimental DTA values of phase transition temperatures (°C) in the $CaCl_2$-$CaSO_4$ system.

$CaSO_4$, mol%	$CaSO_4$, wt%	Eutectic line	Liquidus line	Solid transition
0	0		776	
3.09	3.76	716	768	
5.34	6.47	717	758	
8.49	10.22	720	752	
10.30	12.35	719	738	
12.36	14.75	717		
13.84	16.46	718		
15.30	18.14	716	737	
16.95	20.02	719	744	
20.26	23.76	718	809	
30.10	34.57	717	894	
40.01	45.00	717	970	
50.31	55.40	718	1030	
59.51	64.32	715	1100	
70.02	74.13	714	1176	
74.89	78.53	712	1209	
79.77	82.87	724	1290	1233
88.77	90.65	721	1378	1240
100	100		1510	1220

with their corresponding temperatures of phase transitions summarised in Table 5. The DTA experimental data showed good agreement with literature data [29].

The eutectic transition peak was very intense in both heating and cooling curves for all mixtures. The liquidus transition was not properly visible on the heating curves, which had small and broad peaks, but it was detectable from cooling curves, which nevertheless showed undercooling effect. For mixtures with composition greater than 50 mol % of $CaSO_4$ there was no undercooling effect at the liquidus transition. The transition temperatures for heating and cooling curves for such mixtures coincided in the range of ±5 °C except for the eutectic transition, which still showed undercooling effect. The eutectic mixture was additionally analysed via XRD solely to confirm the absence of any additional phases. These XRD results are provided in the supplementary material (Fig. S 7).

Table 6
Coefficients of the molar heat capacity ($J \bullet mol^{-1} \bullet K^{-1}$) $C_p^\circ = A + B \cdot T + C \cdot T^{-2} + D \cdot T^2$ for the $CaCl_2$(86.0 mol%)-$CaSO_4$(14.0 mol%) mixture taken from DSC measurements.

Temperature range/K	*A*	*B*	*C*	*D*
298–997	78.983	$1.810 \bullet 10^{-3}$	$1.208 \bullet 10^{5}$	$1.749 \bullet 10^{-5}$
997–1050	124.22			

4.3.1. *Thermodynamic properties of the eutectic mixture*

The assumed eutectic mixture $CaCl_2$(86.0 mol%)-$CaSO_4$(14.0 mol %)[2] was chosen to be investigated by DSC in order to collect the corresponding heat capacity and enthalpy of fusion. The mixture was prepared similarly as explained in section 4.2.1. Ten measurements were conducted in total, half of them covering low temperature range (50–690 °C), below the melting temperature, and the other half reaching higher temperatures (50–790 °C), with a mass loss of 0.8 %. The C_p curves are shown in Fig. 4. The coefficients obtained from the heat capacity curves, as measured, are given in Table 6. The eutectic melting temperature derived from DSC analysis was determined to be 724 °C (997 K), which is in good agreement with the value of 718 °C (991 K) obtained from DTA measurements.

Integration of the peak area of phase transition gave the value of enthalpy of fusion. This value was recorded as 30.7 kJ/mol from DSC 404C (10 K/min) and 29.8 kJ/mol from mHTC 96 (4 K/min), with an average value of 30.2 ± 0.5 kJ/mol. Furthermore, the energy calibration method employed in the mHTC 96 device yielded an enthalpy of fusion of 30.2 ± 0.5 kJ/mol. The resulting weighted average value, presented in this work as the final experimental enthalpy of fusion, is 30.2 ± 0.4 kJ/mol.

[2] For all calculations the molar mass M = 114.50 g/mol of the $CaCl_2$(86.0 mol%)-$CaSO_4$(14.0 mol%) mixture was used.

5. Thermodynamic assessment

5.1. $MgCl_2$-$MgSO_4$ system

In this work, the assessment of the binary system $MgCl_2$-$MgSO_4$ was primarily carried out using new experimental data obtained in the present study, while literature data were critically evaluated and only incorporated when consistent with the observed phase equilibria, mainly in the chloride-rich region. Critical thermodynamic information, specifically transition temperatures and enthalpies of the pure sulphates, was previously determined by the same authors in an earlier study [15] and has been incorporated into the current thermodynamic modelling of the binary system. The phase transitions derived from DTA, along with calorimetric measurements from DSC on the eutectic mixture investigated in this study, were integrated into thermodynamic modelling software FactSage. This integration aimed to optimise and enhance the thermodynamic description within the current thermodynamic database. The thermodynamic data on the solution components and the interaction parameters are summarised in Table 7, and the corresponding calculated phase diagram, obtained with the updated thermodynamic database, is presented in Fig. 5. The calculated diagram shows good agreement with the experimental data obtained in this investigation. The discrepancies observed between our measurements and previously reported experimental data [21,22] justified the thermodynamic re-assessment and the subsequent database update presented in this work. The calculated eutectic composition is found to be at 26.3 mol% $MgSO_4$ with a melting temperature of 663 °C (936 K), closely matching the experimentally proposed eutectic composition at 28.0 mol % $MgSO_4$ with a melting temperature of 663 °C (936 K). Additionally, the calculated enthalpy of fusion for the eutectic composition is 40.5 kJ/mol, showing good agreement with the experimentally measured average value of 38.2 ± 1.0 kJ/mol. Fig. S 8 illustrates the comparison of these results with those obtained from commercial database FTsalt [38], highlighting the significant improvement achieved through the current optimisation.

5.2. $CaCl_2$-$CaSO_4$ system

The binary system $CaCl_2$-$CaSO_4$ was assessed by incorporating novel experimental findings acquired during the current investigation, alongside relevant experimental data previously reported in the literature, including the transitions at intermediate sulphate compositions described by Golubeva et al. [29]. The updated thermodynamic optimisation was carried out using experimental phase transition data obtained from DTA and enthalpic measurements derived from DSC, particularly focused on the eutectic composition. These data were integrated into the thermodynamic database. The interaction parameters derived from this assessment are presented in Table 7, while the resultant phase diagram computed using the revised database is depicted in Fig. 6. The calculated phase diagram demonstrates excellent alignment with both the new experimental data presented here and earlier findings from the literature [27,29]. The calculated eutectic composition occurs at approximately 14.2 mol% $CaSO_4$, exhibiting a melting point of 721.5 °C (994.7 K), in agreement with the experimentally observed eutectic composition at 14.0 mol% $CaSO_4$ with a melting temperature of 722 °C (995 K). Moreover, the calculated eutectic enthalpy of fusion is 30.1 kJ/mol, closely aligning with the experimental value of 30.2 ± 0.4 kJ/mol. Fig. S 9 further illustrates a comparison with commercial database FTsalt [38], emphasising the substantial improvements achieved through this advanced optimisation approach.

6. Conclusions

In this work, the phase equilibria of $MgCl_2$-$MgSO_4$ and $CaCl_2$-$CaSO_4$ systems and thermodynamic properties of their eutectic mixtures were studied. Phase diagrams were obtained by DTA investigations conducted in sealed platinum tubes, effectively addressing challenges related to sulphate decomposition and chloride volatilisation.

DTA investigations of the $MgCl_2$-$MgSO_4$ system enabled description of the phase diagram across the entire composition range, revealing significant disparity compared to previously reported literature. This work confirmed $MgCl_2$-$MgSO_4$ to be a single eutectic binary system, with the eutectic composition located near 28.0 mol% $MgSO_4$ and the eutectic temperature at 663 °C (936 K). Through the utilisation of two different DSC devices, the heat capacity of the solid and liquid phases of the eutectic mixture was determined, yielding an enthalpy of fusion of 38.2 ± 1.0 kJ/mol.

Similarly, DTA investigations of the $CaCl_2$-$CaSO_4$ system proved that is a single eutectic system, with the eutectic composition occurring at 14.0 %mol $CaSO_4$ and a corresponding temperature of 722 °C (995 K). DSC measurements reported an enthalpy of fusion for the eutectic mixture of 30.2 ± 0.4 kJ/mol.

Newly obtained experimental data significantly enhance the thermodynamic assessment of the two binary systems studied in this work, culminating in the development of a comprehensive thermodynamic dataset. The calculated results exhibit good agreement with experimental measurements, underpinned by the adoption of only two interaction parameters in the liquid phase for each binary system. Consequently, the dataset provides a comprehensive foundation for thermodynamic modelling across all phases within the systems under investigation, facilitating accurate predictions of thermodynamic properties across their entire composition and temperature ranges. This dataset serves as an important resource for future extensions into multicomponent systems, fostering further advancements in the field.

Table 7
Thermodynamic descriptions of the liquid solution phases.

Gibbs energy data. J/mol	Ref.
Liq: ($MgCl_2$/1.5, $MgSO_4$, $CaCl_2$/1.5, $CaSO_4$)	
${}^{\circ}G_{MgCl_2} = {}^{\circ}G_{MgCl_2(liquid)}$	[16]
${}^{\circ}G_{MgSO_4} = {}^{\circ}G_{MgSO_4(liquid)}$	[15]
${}^{\circ}G_{CaCl_2} = {}^{\circ}G_{CaCl_2(liquid)}$	[48]
${}^{\circ}G_{CaSO_4} = {}^{\circ}G_{CaSO_4(liquid)}$	[20]
$L^{(0)}_{MgSO_4,MgCl_2}$ = -27772.3 + 18*T	a
$L^{(1)}_{MgSO_4,MgCl_2}$ = -2606.47–4.89221*T	a
$L^{(0)}_{CaCl_2,CaSO_4}$ = 35970.8–21.371*T	a
$L^{(1)}_{CaCl_2,CaSO_4}$ = -5159.39–1.5534*T	a

[a] This work.

CRediT authorship contribution statement

Amedeo Morsa: Writing – review & editing, Writing – original draft, Visualization, Validation, Software, Methodology, Investigation, Formal analysis, Data curation, Conceptualization. **Elena Yazhenskikh:** Writing – review & editing, Visualization, Validation, Supervision, Software, Formal analysis, Data curation, Conceptualization. **Rhys Dominic Jacob:** Writing – review & editing, Visualization, Validation. **Michael Müller:** Writing – review & editing, Visualization, Validation, Supervision, Resources, Project administration, Funding acquisition, Formal analysis, Conceptualization. **Dmitry Sergeev:** Writing – review & editing, Visualization, Validation, Supervision, Project administration, Funding acquisition.

Declaration of competing interest

The authors declare that they have no known competing financial interests or personal relationships that could have appeared to influence the work reported in this paper.

Acknowledgements

This work was supported by the Federal Ministry for Economic Affairs and Climate Action on the basis of a decision by the German Bundestag within the project PCM-Screening 2 (FKZ 03EN6005D). Acknowledgment is extended to Mirko Ziegner for assistance with the XRD analyses (see Supplementary Information).

Appendix A. Supplementary data

Supplementary data to this article can be found online at https://doi.org/10.1016/j.calphad.2025.102888.

Data availability

Data will be made available on request.

References

[1] IEA, World Energy Outlook 2021, IEA, Paris, 2021. https://www.iea.org/reports/world-energy-outlook-2021.
[2] D.A. Baharoon, H.A. Rahman, W.Z.W. Omar, S.O. Fadhl, Historical development of concentrating solar power technologies to generate clean electricity efficiently–A review, Renew. Sustain. Energy Rev. 41 (2015) 996–1027.
[3] B. Cárdenas, N. León, High temperature latent heat thermal energy storage: phase change materials, design considerations and performance enhancement techniques, Renew. Sustain. Energy Rev. 27 (2013) 724–737.
[4] M. Liu, W. Saman, F. Bruno, Review on storage materials and thermal performance enhancement techniques for high temperature phase change thermal storage systems, Renew. Sustain. Energy Rev. 16 (4) (2012) 2118–2132.
[5] T. Kousksou, P. Bruel, A. Jamil, T. El Rhafiki, Y. Zeraouli, Energy storage: apllications and challenges, Sol. Energy Mater. Sol. Cell. 120 (2014) 59–80.
[6] M.M. Kenisarin, High-temperature phase change materials for thermal energy storage, Renew. Sustain. Energy Rev. 14 (3) (2010) 955–970.
[7] A. Abhat, Low temperature latent heat thermal energy storage: heat storage materials, Sol. Energy 30 (1983) 313–332.
[8] T. Bauer, D. Laing, R. Tamme, Overview of PCMs for concentrated solar power in the temperature range 200 to 350 C. Advances in Science and Technology, Trans Tech Publ, 2010, pp. 272–277.
[9] M. Liu, E.S. Omaraa, J. Qi, P. Haseli, J. Ibrahim, D. Sergeev, M. Müller, F. Bruno, P. Majewski, Review and characterisation of high-temperature phase change material candidates between 500 C and 700° C, Renew. Sustain. Energy Rev. 150 (2021) 111528.
[10] S.A. Mohamed, F.A. Al-Sulaiman, N.I. Ibrahim, M.H. Zahir, A. Al-Ahmed, R. Saidur, B. Yılbaş, A. Sahin, A review on current status and challenges of inorganic phase change materials for thermal energy storage systems, Renew. Sustain. Energy Rev. 70 (2017) 1072–1089.
[11] M. Sun, T. Liu, H. Sha, M. Li, T. Liu, X. Wang, G. Chen, J. Wang, D. Jiang, A review on thermal energy storage with eutectic phase change materials: fundamentals and applications, J. Energy Storage 68 (2023) 107713.
[12] D. Sergeev, B.H. Reis, I. Dreger, M.t. Baben, K. Hack, M. Müller, Thermodynamics of the Ca(NO3)2 – NaNO3 system, Calphad 67 (2019).
[13] Y. Zhang, X. Zhang, Thermal properties of a new type of calcium chloride hexahydrate-magnesium chloride hexahydrate/expanded graphite composite phase change material and its application in photovoltaic heat dissipation, Sol. Energy 204 (2020) 683–695.
[14] K. Nagano, K. Ogawa, T. Mochida, K. Hayashi, H. Ogoshi, Thermal characteristics of magnesium nitrate hexahydrate and magnesium chloride hexahydrate mixture as a phase change material for effective utilization of urban waste heat, Appl. Therm. Eng. 24 (2–3) (2004) 221–232.
[15] A. Morsa, E. Yazhenskikh, M. Ziegner, E. Wessel, R.D. Jacob, M. Müller, D. Sergeev, Experimental study and thermodynamic assessment of the MgSO4-CaSO4 system, Calphad 90 (2025) 102855.
[16] https://www.enargus.de/pub/bscw.cgi/?op=enargus.eps2&q=PCM-2&v=10&id=2029269.
[17] G.A. Lane, Low temperature heat storage with phase change materials, Int. J. Ambient Energy 1 (3) (1980) 155–168.
[18] D. Sergeev, E. Yazhenskikh, D. Kobertz, K. Hack, M. Müller, Phase equilibria in the reciprocal NaCl–KCl–NaNO3–KNO3 system, Calphad 51 (2015) 111–124.
[19] J. Qi, E. Yazhenskikh, M. Ziegner, X. Zhao, G. Wu, M. Müller, D. Sergeev, Experimental study and thermochemical assessment of the reciprocal system Li+, K+//Cl−, CO32, Calphad 83 (2023) 102603.
[20] E. Yazhenskikh, T. Jantzen, D. Kobertz, K. Hack, M. Müller, Critical thermodynamic evaluation of the binary sub-systems of the core sulphate system Na2SO4–K2SO4–MgSO4–CaSO4, Calphad 72 (2021).
[21] E. Jänecke, Über reziproke salzpaare. II. Das Salzpaar K2Cl2-MgSO4. MgCl2-K2SO4, Z. Phys. Chem. 80 (1912).
[22] E.I. Speranskaya, Exchange decomposition without solvent: irreversible reciprocal system of sodium and magnesium chlorides and sulphates, Bull. Acad. Sci. URSS, Ser. Chim. 2 (1938) 463–487.
[23] R. Nacken, Ueber Langbeinit und Vanthoffit (K2SO4. 2MgSO4 und 3Na2SO4. MgSO4), Nachrichten von der Gesellschaft der Wissenschaften zu Göttingen, Mathematisch-Physikalische Klasse 1907 (1907) 602–613.
[24] A. Ginsberg, Über die Verbindungen von Magnesium-und Natriumsulfat, Z. Anorg. Chem. 61 (1) (1909) 122–136.
[25] J. Rowe, G. Morey, C. Silber, The ternary system K2SO4•MgSO4•CaSO4, J. Inorg. Nucl. Chem. 29 (1967) 925–942.
[26] O. Sackur, Geschmolzene salze als Lösungsmittel: Erwiderung an herrn WC bray, Zeitschrift für Physikalische Chemie 80 (1) (1912), 254-254.
[27] A.M. Pichugin, Technical Encyclopedia- special communication (n.d.): 7: 192. Appears, in: N. K. Voskresenskaya Compilers, N.K. Voskresenskaya, N.N. Evseeva, S.I. Berul, I.P. Vereshchetina (Eds.), Schmorak J. CaCl2-CaSO4 in Handbook of Solid-Liquid Equilibria in Systems of Anhydrous Inorganic Salts, 1970. Volume I: 628.
[28] E. Jänecke, W. Mühlhäusser, Das reziproke Salzpaar (K2-Ca)(Cl2-SO4), Z. Anorg. Allg. Chem. 228 (1936) 241–248.
[29] M.S. Golubeva, A.G. Bergman, The ternary reciprocal system of the chlorides and sulfates of potassium and calcium, Russ. J. Gen. Chem. 26 (1956) 249–258.
[30] A. Palkin, Evolution of the diagram of state of ternary reciprocal systems in the absence of water, Izvestiya Sektora Fiziko-Khimicheskogo Analiza, Institut Obshchei i Neorganicheskoi Khimii, Akademiya Nauk SSSR 17 (1949) 228–253.
[31] T.D. Zimina, A.G. Bergman, G.I. Nagornyi, The Ba, Ca, Na//Cl, SO4 reciprocal system, Russ. J. Inorg. Chem. 10 (1965) 1167–1171.
[32] P.A. Arbukhanova, Y.A. Dibirov, N.N. Verdiev, A.M. Amadziev, The CaF2-CaCl2-CaSO4 system, Russ. J. Inorg. Chem. 54 (6) (2009) 980–982.
[33] T.D. Zimina, A.G. Bergaman, G.I. Nagornyi, Vzaimnaya sistema iz khloridov i sul'fatov natriya. kal'tsiya i bariya, Zhur. Neorg. Khimii 10 (9) (1965) 2145–2151.
[34] J. Rowe, G. Morey, I. Hansen, The binary system K2SO4-CaSO4, J. Inorg. Nucl. Chem. 27 (1965) 53–58.
[35] A.S.f. Testing, Materials, Standard Test Method for Determining Specific Heat Capacity by Differential Scanning Calorimetry, ASTM International2011.
[36] D. Ditmars, S. Ishihara, S. Chang, G. Bernstein, E. West, Enthalpy and heat-capacity standard reference material: synthetic sapphire (α-Al2O3) from 10 to 2250 K, J. Res. Natl. Bur. Stand. 87 (2) (1982) 159.
[37] H. Lukas, S.G. Fries, B. Sundman, Computational Thermodynamics: the Calphad Method, Cambridge University Press, 2007, p. 104.
[38] C.W. Bale, E. Bélisle, P. Chartrand, S.A. Decterov, G. Eriksson, A.E. Gheribi, K. Hack, I.H. Jung, Y.B. Kang, J. Melançon, A.D. Pelton, S. Petersen, C. Robelin, J. Sangster, P. Spencer, M.A. Van Ende, FactSage thermochemical software and databases, 2010–2016, Calphad 54 (2016) 35–53.
[39] FactSage, Facility for the analysis of chemical thermodynamics, Available from:, Version 8.3. http://www.factsage.com/.
[40] T.M. Besmann, K.E. Spear, Thermochemical modeling of oxide glasses, J. Am. Ceram. Soc. 85 (12) (2002) 2887–2894.
[41] E. Yazhenskikh, K. Hack, M. Müller, Critical thermodynamic evaluation of oxide systems relevant to fuel ashes and slags. Part 1: alkali oxide–silica systems, Calphad 30 (3) (2006) 270–276.
[42] Database GTOx, GTT-Technologies, Forschungszentrum Jülich, 2010-2020, GTT-technologies.
[43] B. Reis, F. Tang, P. Keuter, M. to Baben, User-friendly and robust Calphad optimizations using Calphad Optimizer in FactSage, Calphad 88 (2025) 102800.
[44] N.B.S. US, Selected values of chemical thermodynamic properties, Circ 500 (1952).
[45] V. Glushko, Termicheskie konstanty (thermal constants of substances), in: Online Reference Book, Moscow State University, Chemical Department, Moscow, 1982. http://www.chem.msu.ru/cgi-bin/tkv.pl?show=welcome.html(1965-1982.
[46] M.W. Chase, N.I.S. Organization, NIST-JANAF thermochemical tables, Am Chem. Soc. Washington, DC1998.
[47] G. Moore, Heat contents at high temperatures of the anhydrous chlorides of calcium, iron, magnesium and Manganese 1, J. Am. Chem. Soc. 65 (9) (1943) 1700–1703.
[48] B.H. Reis, Development of a Novel Thermodynamic Database for Salt Systems with Potential as Phase Change Materials, BTU Cottbus-Senftenberg, 2021.
[49] I. Barin, G. Platzki, Thermochemical Data of Pure Substances, Wiley Online Library, 1989.
[50] M. Tokareva, The reciprocal system of nitrates and chlorides of lithium and calcium, J. Inorg. Chem. 2 (7–9) (1957) 230.
[51] D.W. Green, R.H. Perry, Perry's Chemical Engineers' Handbook, McGraw-Hill Education, 2008.
[52] (V13.1), SGPS - SGTE Pure Substances Database, 2019.
[53] A. Obaied, F. Tang, I. Roslyakova, M. to Baben, "2 1/2th" generation Calphad databases: extrapolating heat capacities of elements and compounds to 0K, Calphad 75 (2021) 102352.
[54] R.A. Robie, S. Russell-Robinson, B.S. Hemingway, Heat capacities and entropies from 8 to 1000 K of langbeinite (K2Mg2 (SO4) 3), anhydrite (CaSO4) and of gypsum (CaSO4· 2H2O), Thermochim. Acta 139 (1989) 67–81.
[55] K. Grjotheim, J.L. Holm, J. Malmo, The phase diagram of the system MgCl2-CaCl2, and thermo-dynamic properties of molten mixtures in this system, Acta Chem. Scand. 24 (1970) 77–86.
[56] E. Dewing, F. Richardson, Decomposition equilibria for calcium and magnesium sulphates, Trans. Faraday Soc. 55 (1959) 611–615.
[57] E. Jänecke, Über das Schmelz-und Erstarrungsbild des doppelt-ternären Systemes (K2· Na2· Mg)(Cl2· SO4), Z. Anorg. Chem. 261 (3-4) (1950) 213–225.
[58] W. Grahmann, Vergleich der Sulfate der Erdalkalien und des Bleis in den Temperatur-Konzentrationsdiagrammen mit Kaliumsulfat unter besonderer Berücksichtigung der Dimorphie von Anhydrit. Colestin, Baryt Und Anglesit, 1913. Voss.

[59] A. Bellanca, L'aftitalite nel sistema ternario K2SO4-Na2SO4-CaSO4, Period. Mineral. 13 (1942) 21–86.
[60] J. Torres, J. Mendez, M. Sukiennik, Transformation enthalpy of the alkali-earths sulfates (SrSO4, CaSO4, MgSO4, BaSO4), Thermochim. Acta 334 (1–2) (1999) 57–66.
[61] C. Pistorius, J. Boeyens, J. Clark, Phase diagrams of NaBF 4 and NaClO 4 to 40 kbar and the crystal-chemical relationship between structures of CaSO 4, AgMnO 4, BaSO 4 and high-NaClO 4, High. Temp. - High. Press. 1 (1969) 41–52.
[62] F. Tesfaye, D. Lindberg, L. Hupa, The K 2 SO 4–CaSO 4 system and its role in fouling and slagging during high-temperature processes. Materials Processing Fundamentals 2018, Springer, 2018, pp. 133–142.
[63] D. Kobertz, M. Müller, Experimental studies and Re-assessment of the quasi-binary systems containing the sulfates of sodium, potassium, and calcium by differential thermal analysis and X-Ray diffraction in CALPHAD XLCALPHAD XL, 2011.
[64] P. Coursol, A. Pelton, P. Chartrand, M. Zamalloa, The CaSO4-Na2SO4-CaO phase diagram, Can. Metall. Q. 44 (4) (2005) 537–546.